ROBUST AUTOPILOT DESIGN STRATEGY FOR FUNCTIONALLY DEPENDENT PARAMETER UNCERTAINTIES

Guy E. Shaviv* Moshe Idan†
Department of Aerospace Engineering
Technion - Israel Institute of Technology, Haifa 32000, Israel

Abstract

In this paper an approach is presented to incorporate known functional dependencies of model parameters on uncertain physical quantities. The approach is suitable in cases where the source of the plant uncertainty is mainly accountable by a few unknown physical parameters. In such cases, uncertainty over-bounding is greatly reduced compared to using general uncertainty descriptions. This may lead to a better performance/robustness trade-off in a robust controller design. The basis of the approach is to describe the model uncertainties in the unknown physical parameters as Linear Fractional Transformations (LFTs). Then, using LFT algebra, a LFT is obtained, which describes the effect of the uncertain variables on the plant model. The resulting model can be used with several robust control synthesis techniques. In particular, in this paper μ synthesis, which is most suitable for the resulting functional dependence model was adopted. As an example, an aircraft controller to follow roll angle commands while keeping the lateral acceleration close to zero was designed. The resulting controller satisfies the specified performance requirements and its superior characteristics is demonstrated by comparison to a controller which was designed using general uncertainty bounds model.

1 Introduction

Autopilot design is often based on a linear model of an aircraft, the numerous parameters of which depend dominantly on a few unknown physical quantities such as the location of the vehicle center of gravity (c.g.), the air density, the trim angle of attack and the Mach number. Some of these dependencies may be modeled analytically in a relatively simple form (e.g., the model coefficients dependence on the aircraft c.g. location or on the air density,) while others may be more difficult to model analytically, but still could be expressed empirically based on experimental results. The design goal is to achieve robust performance for the uncertainties in these few physical quantities. In this work, the effect of additional model uncertainties that are not related to any common physical quantity, such as uncertainties in the non dimensional aerodynamic stability and control derivatives, are assumed to be small compared to those caused by the uncertainties in the above mentioned physical quantities, and thus are not discussed here.

A problem, closely related to the one presented above, can be formulated when designing an autopilot for several flight conditions. The flight conditions are often defined by different values of some physical parameters, such as flight altitude and speed. These parameters, which affect the linear model of the aircraft , can be considered unknown and allowed to perturb within a specified range of interest. The requirement for the controller to operate at all the conditions is equivalent to the requirement to provide robust stability and performance of the system while the physical parameters vary in the given range.

In order to achieve strict performance requirements, it is necessary to take into account the uncertainty in the system model and the manner by which the uncertain variables affect the system model parameters. Several approaches exist for describing the system uncertainty for use in robust control design. The multi-model approach (see Ref. 1 and references therein) evaluates the system at several operating points and attempts to find a controller that meets performance criteria for all system models simultaneously. The complexity of this approach increases with the number of uncertainty and controller parameters, which makes it difficult to implement beyond very few of these parameters. In addition, there is no guarantee on the performance at operating points not considered in the design. Alternatively, there are design techniques that account for the model uncertainties by specifying general bounds on their overall effect on the plant frequency response. The design goal in such methods is to minimize a frequency weighted sensitivity function, leading to design techniques like H_∞.[2,3] An additional approach is to specify bounds

*Graduate Student
†Annie and Charles Corrin Academic Lecturer

on each of the model coefficients,[4-6] which is usually applied with μ synthesis.

The drawback of the latter methods for uncertainty modeling is that they do not incorporate the exact functional dependence (if such exists) of the model parameters on a few uncertain variables. Instead, a more general uncertainty space is defined, often over-bounding the true uncertainty space. In H_∞ this over-bounding results from ignoring phase or structure information, while in parameter bounding μ it is caused by ignoring parameter dependency information. This over-bounding may lead to conservative controller design and prevent the autopilot from achieving the desired performance in the entire uncertainty range considered, as will be demonstrated throughout this paper.

In this paper we present a design methodology for incorporating the known functional dependence of the model coefficients on physical parameters into the uncertainty model, resulting in a less restrictive uncertainty model. While the resulting model can be used for controller design using any robust control technique, the μ synthesis is adopted here since it best fits the structured uncertainty model obtained.

The advantages of the new technique were recently demonstrated for a SISO example with only one uncertain physical parameter.[7] In this work we tackle a more realistic MIMO case with a few uncertain physical parameters, where the advantages of the proposed technique are expected to be even more pronounced. A model for the lateral dynamics of a Remotely Piloted Vehicle (RPV) with unknown payload mass and varying flight altitude, modeled as unknown air density, is constructed. The goal is to design a robust lateral autopilot for the unknown aircraft mass which can operate at an altitude range of interest, thus avoiding controller gain scheduling. To demonstrate the superior performance of the autopilot designed it is compared to controllers obtained using other robust control design methods.

In the next section we discuss the underlying concept of the robust controller design approach. In section 3 an application of the proposed approach is demonstrated by developing an uncertainty model of a RPV carrying a payload of unknown mass and operating at a certain range of altitudes. A μ controller is designed using this model in section 4 and is compared to a controller which was designed using a standard uncertainty model in section 5. Summary and conclusions are presented in section 6.

2 The Concept

The controller design process is often based on a model of the dynamic system. Since the dynamic characteristics of the physical system may be different than its model, it is said that the system model has an uncertainty. In such cases, a robust controller has to be designed to achieve specified performance qualities for the entire uncertainty space of the system model. In this paper we treat systems with uncertainties dominated by a few uncertain physical parameters. It is assumed that these unknown physical parameters change the model of the system in a known manner.

Not taking into account the resulting dependencies between the model parameters may lead to an uncertainty space over-bounding, as is demonstrated for a two parameter example in Fig. 1. Here the two model

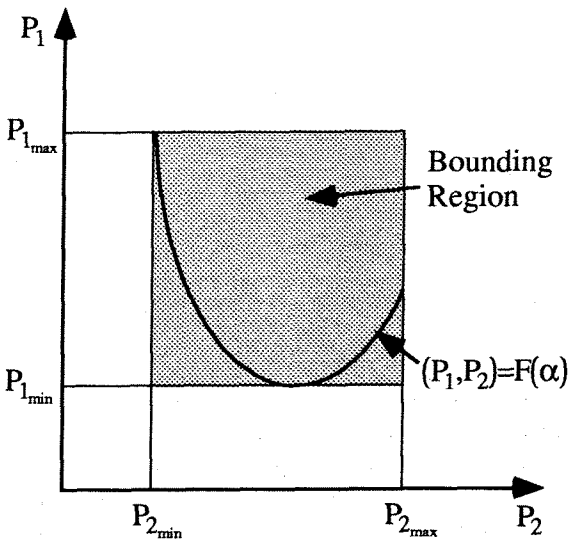

Figure 1: Parameters with Functional Dependence and a Possible Uncertainty Bounding

parameters (P_1, P_2) are assumed to depend on a single uncertain physical quantity α. As α varies, P_1 and P_2 vary simultaneously, making them dependent. A simple way to define the uncertainty space could be to bound the perturbation range of each of the parameters separately (the gray area in Fig. 1). This of course will result in an over-bounding of the uncertainty space. When using these bounds in the robust controller design, the most difficult design point in the uncertainty space may correspond to a non physical parameter combination, for which the desired performance criteria could be difficult or even impossible to meet. The use of the functional dependence between the parameters provides information, for example, that when P_1 is maximal, P_2 obtains a specific value within the range of its variation. Consequently, there is no need to design a controller for a combination in which both parameters are at their maximal values. The use of the parameter functional dependence eliminates uncertainty over-bounding by describing the uncertainty space in an exact manner, letting the controller tackle physical cases only.

We use a recently presented modeling scheme for a system with uncertainty which is governed by a small number of unknown physical parameters.[7] The method

is based on incorporating the known functional dependence of the model coefficient on the unknown physical parameters into the uncertainty model, thus avoiding undesired uncertainty over-bounding. This may potentially lead to a better trade-off between performance and robustness at the design stage, and reduce the design problem complexity as the dimension of the unknown physical parameters is usually smaller compared to the number of model parameters affected by them. Ref. 7 presents the method, underlying principles and algebra. In this paper we focus on demonstrating the use of the approach by building a functional dependence uncertainty model for a more realistic and complex autopilot design example.

During the modeling process, the relations between each uncertainty variable and the model parameters is often known. The procedure is to express these basic uncertainties of each of the model parameters as a LFT and then, using LFT algebra, the complete uncertainty model, which describes the effect of each uncertainty variable on the model, is derived. The basics of LFT algebra is reviewed in Ref. 8. This modeling procedure leads to an uncertainty model presented in an analytical form. Hence, the LFT algebra is performed analytically. For this purpose, a symbolic LFT manipulation package was developed under the *Mathematica™* environment, which enables to perform symbolic LFT algebra.

The resulting uncertainty model is a LFT, which contains only physical uncertainties in its uncertainty block. Due to inner structure of the plant and the modeling procedure, some of the physical uncertainties will be repeated, i.e. will have several instances in the uncertainty block. These repeated uncertainties are called "repeated scalar blocks". Some of these repetitions are caused by the modeling procedure and are superfluous. They are introduced in much the same way as excess modes may be created when cascading two systems in a state space realization. Often these repetitions could be eliminated by finding a "minimal realization" for the LFT. This is similar to finding a minimal realization of multi dimensional systems[9] with respect to the repeated uncertainties. The difficulty in achieving a minimal realization is that, except for a few special cases, a general solution for this problem does not exist.[8]

After an uncertainty model is obtained, any robust control design method, which can handle structured uncertainties, may be used to synthesis a controller. In this paper, μ synthesis was applied,[10] since it comes naturally with the LFT syntax, and it best suites the resulting structured uncertainty model. The modeling and controller design procedures are presented in detail for an autopilot design example in the next section.

3 Aircraft Model

As a first step in a robust autopilot design for a RPV, a model of its lateral dynamics and the uncertainty model are developed in this section. The RPV is assumed to carry a payload of an unknown mass, hanged from a given point on the RPV. The change in the payload mass, changes therefore, the aircraft's total mass and the location of the center of gravity (c.g.) This changes the dynamic characteristics of the aircraft. Additionally, the aircraft is required to operate at an altitude range from 0 to 10 Kft (about 3 Km). The change in altitude changes the air density, which in turn changes the aerodynamic characteristics of the aircraft. Thus, the aircraft model has two physical variables governing its uncertainty: the aircraft mass and the air density. The aircraft and payload data used are of the Israel Aircraft Industries (IAI) *"Pioneer"* RPV.

The Uncertainty Model

The change in the RPV payload mass affects both the total aircraft mass and the c.g. location of the aircraft/payload system. The change in the RPV flight altitude changes the air density. We will first describe the uncertainty in these basic model parameters as LFTs, which will then be used in the sequel to obtain an uncertainty model of the aircraft equations of motion.

The change in aircraft mass can be modeled as a multiplicative uncertainty by

$$m = \hat{m}(1 + \delta_m) \tag{1}$$

which can be expressed as a LFT

$$m = \mathcal{F}_l\left(\begin{bmatrix} \hat{m} & \hat{m} \\ 1 & 0 \end{bmatrix}, \delta_m\right) \tag{2}$$

The uncertainty variable δ_m represents the relative change in the aircraft mass due to a change in the payload mass. $\hat{m}$ is the nominal mass.

In this example the payload is located at a known location along the x axis of that system. Thus the change in the payload mass shifts the c.g. in the x direction only. The relation between δ_{cg}, the shift in the x position of the c.g. from its nominal position, and δ_m can be expressed as

$$\delta_{cg} = \frac{(x_{pl} - \hat{x}_{cg})\delta_m}{1 + \delta_m} \tag{3}$$

where x_{pl} is the known payload location along the x axis and $\hat{x}_{cg}$ is the nominal c.g. location. Eq. (3) can be written as a LFT

$$\delta_{cg} = \mathcal{F}_l\left(\begin{bmatrix} 0 & \bar{x}_{pl} \\ 1 & -1 \end{bmatrix}, \delta_m\right) \tag{4}$$

where $\bar{x}_{pl} \triangleq x_{pl} - \hat{x}_{cg}$ is the distance between the payload location and the nominal c.g. location.

It will be noted that the shift in the c.g. along the x axis affects also the aircraft's moments of inertia I_{zz} and I_{xz}. However, it was found that the total change in the moments of inertia due to the payload mass range considered is less then 2% and was therefore neglected. The main effect of the mass uncertainty is on the yaw moment and the lateral acceleration equations, as presented in the sequel.

The change in flight altitude changes the air density ρ. This change can be expressed as a multiplicative uncertainty

$$\rho = \hat{\rho}(1 + \delta_\rho) \tag{5}$$

where $\hat{\rho}$ is the air density at the nominal flight altitude and δ_ρ its relative uncertainty. This can be expressed as a LFT

$$\rho = \mathcal{F}_l\left(\begin{bmatrix} \hat{\rho} & \hat{\rho} \\ 1 & 0 \end{bmatrix}, \delta_\rho\right) \tag{6}$$

Linear Model of the Aircraft Lateral Dynamics

The aircraft equations of motions are described in the stability coordinate system,[11] with its origin at the aircraft center of gravity. The linear model of the lateral dynamics of an aircraft perturbed from straight and level trim flight includes four perturbation variables: β - the side slip angle, p - the roll rate, r - the yaw rate and ϕ - the roll angle, arrange in a state vector in this order. The differential equations for these variables are given by[12]

$$\dot{\beta} = Y_v\beta + r - \frac{g}{U}\phi + Y_{\delta_r}\delta_r \tag{7a}$$

$$\dot{p} = \frac{I_{xz}}{I_{xx}}\dot{r} + L_\beta\beta + L_p p + L_r r + L_{\delta_a}\delta_a + L_{\delta_r}\delta_r \tag{7b}$$

$$\dot{r} = \frac{I_{xz}}{I_{zz}}\dot{p} + N_\beta\beta + N_p p + N_r r + N_{\delta_a}\delta_a + N_{\delta_r}\delta_r \tag{7c}$$

$$\dot{\phi} = p \tag{7d}$$

Here U is the trim flight velocity. $Y_{(\cdot)}$, $L_{(\cdot)}$ and $N_{(\cdot)}$ are the dimensional derivatives for the side force and the roll and yaw moments, respectively, and are defined as

$$Y_{(\cdot)} \triangleq \frac{1}{m}\frac{\partial Y}{\partial(\cdot)} \qquad L_{(\cdot)} \triangleq \frac{1}{I_{xx}}\frac{\partial L}{\partial(\cdot)} \qquad N_{(\cdot)} \triangleq \frac{1}{I_{zz}}\frac{\partial N}{\partial(\cdot)} \tag{8}$$

v is the lateral velocity given by $v = \beta U$. In these equations a linear dependence is assumed between (Y, L, N) and model states and the control variables.

The control inputs in Eqs. (7) are the aileron δ_a and the rudder δ_r deflections. The measurements which are available for the controller are p, r and $a_{y_{cg}}$, the lateral acceleration at the c.g. location, given by

$$a_{y_{cg}} = \dot{v} - g\phi \tag{9}$$

The linear equations of motion (7) together with lateral acceleration, roll rate and yaw rate measurements, can be expressed as a transfer function

$$\begin{Bmatrix} a_y^m(s) \\ p(s) \\ r(s) \end{Bmatrix} = \mathcal{P}(s) \begin{Bmatrix} \delta_a(s) \\ \delta_r(s) \end{Bmatrix} \tag{10a}$$

$$\mathcal{P}(s) = \left[\begin{array}{cccc|cc} Y_v & 0 & -1 & \frac{g}{U} & 0 & Y_{\delta_r} \\ L'_\beta & L'_p & L'_r & 0 & L'_{\delta_a} & L'_{\delta_r} \\ N'_\beta & N'_p & N'_r & 0 & N'_{\delta_a} & N'_{\delta_r} \\ 0 & 1 & 0 & 0 & 0 & 0 \\ \hline a_{y_\beta} & a_{y_p} & a_{y_r} & -g & a_{y_{\delta_a}} & a_{y_{\delta_r}} \\ 0 & 1 & 0 & 0 & 0 & 0 \\ 0 & 0 & 1 & 0 & 0 & 0 \end{array}\right] \tag{10b}$$

where $\left[\begin{array}{c|c} \cdot & \cdot \\ \hline \cdot & \cdot \end{array}\right]$ denotes a transfer function with a state space realization as follows

$$G(s) = \left[\begin{array}{c|c} A & B \\ \hline C & D \end{array}\right] \triangleq D + C(sI - A)^{-1}B \tag{11}$$

which, expressed as a LFT becomes:

$$G(s) = \mathcal{F}_u\left(\begin{bmatrix} A & B \\ C & D \end{bmatrix}, \frac{1}{s}I\right). \tag{12}$$

Hence, Eq. (10) can also be written as

$$\mathcal{P}(s) = \mathcal{F}_u\left(\mathcal{P}_{lat}, \frac{1}{s}I_4\right) \tag{13}$$

where $\mathcal{P}_{lat}$ is the lateral dynamics matrix $\mathcal{P}_{lat} = \begin{bmatrix} A & B \\ C & D \end{bmatrix}$ and (A, B, C, D) are the state space realization matrices of the lateral dynamics model of the aircraft. In these equations, the weighted dimensional derivatives $L'_{(\cdot)}$ and $N'_{(\cdot)}$ are defined as

$$L'_{(\cdot)} \triangleq \frac{1}{I_c}\left(L_{(\cdot)} + \frac{I_{xz}}{I_{xx}}N_{(\cdot)}\right) \tag{14a}$$

$$N'_{(\cdot)} \triangleq \frac{1}{I_c}\left(N_{(\cdot)} + \frac{I_{xz}}{I_{zz}}L_{(\cdot)}\right) \tag{14b}$$

and $I_c = 1 - I_{xz}^2/I_{xx}I_{zz}$.

Equations (7) and (9) are written with respect to the *unknown* true c.g. location of the aircraft. As the payload mass changes, the c.g. location changes with it. In order to accommodate for this change, the aerodynamic forces and moments, which are normally expressed with respect to the a fixed reference point (usually the nominal c.g.), must be corrected.

First, the side slip angle β at the reference point should be corrected to reflect its change due to the yaw rate times the distance between the nominal and true c.g. locations. However, since the objective of the controller is to minimize lateral acceleration, the value of the lateral velocity and its derivatives are expected to be small, and hence this correction is neglected for simplicity. Consequently, since in our case the c.g. variations are along the x axis, only the yaw moment equations have to be corrected. The yaw moment N at the

unknown true c.g. location relates to the yaw moment $\hat{N}$ at the nominal c.g. location according to

$$N = \hat{N} + Y\delta_{cg} \tag{15}$$

where Y is the side force at the nominal c.g.

The lateral accelerometer is installed at a fixed body position in the aircraft which is assumed to be at the nominal c.g. location. When the true c.g. location changes, this accelerometer measures an acceleration a_y^m which has a component due to the yaw rate and is given by

$$a_y^m = a_{y_{cg}} + \delta_{cg}\dot{r} \tag{16}$$

where $a_{y_{cg}}$ is the acceleration at the true c.g. location.

Using the corrections of Eqs. (15) and (16) and the uncertainties in m, c.g. location and ρ of Eqs. (2),(4) and (6), the aircraft uncertainty model due to δ_m and δ_ρ can be constructed. In this work this is done sequentially: first the model for δ_m is derived and then the effects of δ_ρ are incorporated.

By using the definitions in Eq. (8) and applying the corrections due to the uncertainty in the mass and the c.g. position, Eqs. (2), (4) and (15), it is possible to obtain LFT expressions for the effect of the uncertainty in payload mass on the dimensional aerodynamic derivatives. This is achieved by performing the implied differentiations of Eq. (8) using the relations of Eqs. (2) and (15) and then replacing δ_{cg} with its LFT expression in Eq. (4). After some algebraic LFT manipulations,[7,8] which in this work was performed by a symbolic package for *Mathematica*™, the result is:

$$Y_v = \mathcal{F}_l\left(\begin{bmatrix} \hat{Y}_v & 1 \\ -\hat{Y}_v & -1 \end{bmatrix}, \delta_m\right) \tag{17a}$$

$$Y_{\delta_r} = \mathcal{F}_l\left(\begin{bmatrix} \hat{Y}_{\delta_r} & 1 \\ -\hat{Y}_{\delta_r} & -1 \end{bmatrix}, \delta_m\right) \tag{17b}$$

$$N_\beta = \mathcal{F}_l\left(\begin{bmatrix} \hat{N}_\beta & 1 \\ \frac{C_{Y_\beta}\rho SU\bar{x}_{pl}}{2I_{zz}} & -1 \end{bmatrix}, \delta_m\right) \tag{17c}$$

$$N_{\delta_r} = \mathcal{F}_l\left(\begin{bmatrix} \hat{N}_{\delta_r} & 1 \\ \frac{C_{Y_{\delta_r}}\rho SU\bar{x}_{pl}}{2I_{zz}} & -1 \end{bmatrix}, \delta_m\right) \tag{17d}$$

where $\hat{(\cdot)}$ denotes nominal values. C_{Y_β} and $C_{Y_{\delta_r}}$ are the non-dimensional stability derivatives, defined in term of the dimensional derivatives as:

$$C_{Y_\beta} \triangleq Y_v\frac{2m}{\rho SU} \qquad C_{Y_{\delta_r}} \triangleq Y_{\delta_r}\frac{2m}{\rho SU} \tag{18}$$

where S is the reference wing area. Other dimensional aerodynamic derivatives are not affected by δ_m.

The measured lateral acceleration can be expressed as a LFT with a repeated scalar block of order two containing the mass uncertainty, by using Eqs. (9) and (16), substituting $\dot{v}$ and $\dot{r}$ with Eqs. (7a) and (7c) and including the LFTs from Eqs. (2) and (4) to obtain Eq. (19) in which $c_1 = \frac{\rho SU\bar{x}_{pl}}{2I_cI_{zz}}$.

By substituting the LFTs of Eqs. (17) and (19) into the transfer function of Eq. (10), collecting the uncertainty blocks into a single block and minimizing its dimension, the lateral dynamics model is obtained as a LFT of the mass uncertainty. This model has a third order repeated scalar uncertainty block and is given by Equations (20) describe exactly the effect of the mass uncertainty on the lateral dynamics model of the aircraft.

Now the uncertainty in the air density is incorporated. Equations (20) contain expressions, such as all the dimensional derivatives, which depend on the air density. By writing explicit expressions for the dimensional derivatives and substituting the uncertain air density with its LFT expression of Eq. (6), a linear dynamic model is obtained as a LFT, which depends on the uncertainties in the mass and the air density. After combining the δ_ρ uncertainty blocks of the elements of M_{lat} and reducing the dimension of the resulting block, a δ_ρ repeated scalar block of three is obtained

$$\mathcal{P}'_{lat} = \mathcal{F}_l\left(M'_{lat}, \mathrm{diag}\left\{\delta_\rho I_3, \delta_m I_3\right\}\right) \tag{21}$$

where $\mathcal{P}'_{lat}$ is the resulting lateral dynamics system matrix. The analytical expression for M'_{lat} is quite complex and thus only its numeric form for the *"Pioneer"* RPV is given in the appendix.

The model in Eq. (21) describes the effect of the two uncertain variables, the mass and the air density, on the linear model of the lateral dynamics of the aircraft. One could now include additional model uncertainties due to other sources of parametric uncertainty, such as then trim angle of attack. Also, unstructured uncertainties could be added if their analytic dependencies are difficult to obtain.

Here we would like to stress that it would be beneficial to construct a functional dependence uncertainty models even when only a part of the uncertainty can be expressed as parameter dominated. The portion of the uncertainty which cannot be accounted by parameter functional dependence can be modeled as unstructured by applying general bounds. This way uncertainty overbounding is reduced, since the unstructured portion of the uncertainty is smaller and does not have to account for the entire uncertainty space.

A functional dependence uncertainty model can also be created when there is no analytical knowledge of the parameter dependence, but an empirical relation may be found. These empirical relations between parameters can be computed by fitting experimental data with rational functions, which can then be used to construct functional dependence uncertainty models.

The model presented is Eq. (21) is now incorporated in a μ synthesis stage to design a controller which is robust to changes in these uncertain variables and meets

$$a_y^m = \mathcal{F}_l\left(\left[\begin{array}{cccccc:cc} \hat{Y}_v & 0 & 0 & -g & 0 & \hat{Y}_{\delta_r} & \bar{x}_{pl} & 0 \\ \hat{N}'_\beta - \frac{\hat{Y}_v}{\bar{x}_{pl}} & \hat{N}'_p & \hat{N}'_r & 0 & \hat{N}'_{\delta_a} & \hat{N}'_{\delta_r} - \frac{\hat{Y}_{\delta_r}}{\bar{x}_{pl}} & -1 & -1 \\ C_{Y_\beta} c_1 & 0 & 0 & 0 & 0 & C_{Y_{\delta_r}} c_1 & 0 & -1 \end{array}\right], \delta_m I_2\right)\left\{\begin{array}{c} \beta \\ p \\ r \\ \phi \\ \delta_a \\ \delta_r \end{array}\right\} \tag{19}$$

$$\mathcal{P}_{lat} = \mathcal{F}_l\left(M_{lat}, \delta_m I_3\right) \tag{20a}$$

$$M_{lat} = \left[\begin{array}{cccccc:ccc} \hat{Y}_v & 0 & -1 & \frac{g}{U} & 0 & \hat{Y}_{\delta_r} & 1 & 0 & 0 \\ \hat{L}'_\beta & \hat{L}'_p & \hat{L}'_r & 0 & \hat{L}'_{\delta_a} & \hat{L}'_{\delta_r} & 0 & 1 & 0 \\ \hat{N}'_\beta & \hat{N}'_p & \hat{N}'_r & 0 & \hat{N}'_{\delta_a} & \hat{N}'_{\delta_r} & 0 & \frac{I_{xx}}{I_{xz}} & 0 \\ 0 & 1 & 0 & 0 & 0 & 0 & 0 & 0 & 0 \\ \hat{Y}_v & 0 & 0 & -g & 0 & \hat{Y}_{\delta_r} & 0 & 0 & 1 \\ 0 & 1 & 0 & 0 & 0 & 0 & 0 & 0 & 0 \\ 0 & 0 & 1 & 0 & 0 & 0 & 0 & 0 & 0 \\ \hdashline \hat{Y}_v & 0 & 0 & 0 & 0 & \hat{Y}_{\delta_r} & -1 & 0 & 0 \\ C_{Y_\beta} c_1 \frac{I_{xx}}{I_{zz}} & 0 & 0 & 0 & 0 & C_{Y_{\delta_r}} c_1 \frac{I_{xx}}{I_{zz}} & 0 & -1 & 0 \\ \hat{N}'_\beta \bar{x}_{pl} - \hat{Y}_v & \hat{N}'_p \bar{x}_{pl} & \hat{N}'_r \bar{x}_{pl} & 0 & \hat{N}'_{\delta_a} \bar{x}_{pl} & \hat{N}'_{\delta_r} \bar{x}_{pl} - \hat{Y}_{\delta_r} & 0 & \frac{I_{xx} \bar{x}_{pl}}{I_{zz}} & -1 \end{array}\right] \tag{20b}$$

stringent performance requirements, as presented in the next section.

4 Autopilot Design

In this section the design of a robust autopilot for the *"Pioneer"* RPV model derived in the previous section is presented. The controller is designed using μ synthesis with the objectives of following roll angle commands while keeping the lateral acceleration of the aircraft minimal. The autopilot is required to operate at an altitude range between 0 and 10 Kft (3 Km) above sea level, at a constant velocity of 40 m/s. The aircraft has a nominal mass of 167 kg and carries payloads ranging from 0 to 60 kg. The controller inputs are the measured roll and yaw rates and the lateral acceleration at the nominal c.g.. The controller outputs are aileron and rudder commands.

The μ synthesis technique is applied to an interconnection model, which includes frequency domain weighting functions to specify the robustness and performance requirements. The complete interconnection model used for the μ design of the RPV autopilot is given in Fig. 2.

The controller is designed to implicitly follow a roll angle model, described as a second order system[12]

$$W_{ref} = \frac{\omega_p^2}{s^2 + 2\zeta_p \omega_p s + \omega_p^2} \tag{22}$$

where $\omega_p = 1$ rad/sec and $\zeta_p = 0.5$. The tracking error between the aircraft roll angle and the reference model is required to be less than 0.1 degree in steady state and is less important at high frequencies. Hence a weight

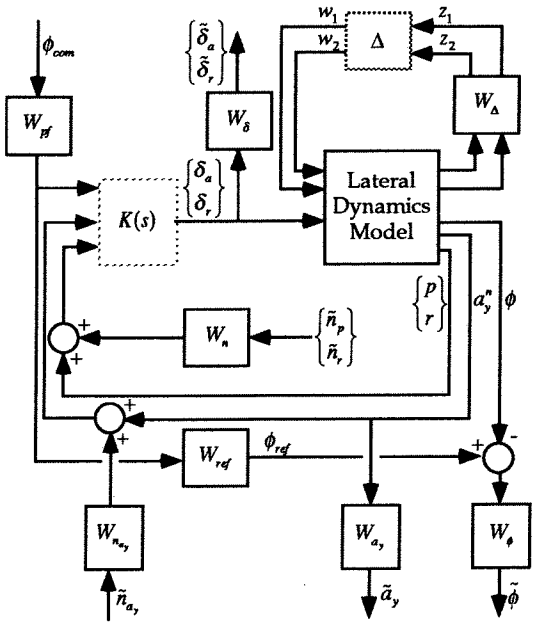

Figure 2: Interconnection Model for μ Design

on the tracking error was set to

$$W_\phi = \frac{180}{0.1\pi} \frac{s/10+1}{s/6+1} \tag{23}$$

The control objective is to perform the bank without developing lateral acceleration, i.e., perform a coordinated turn. The lateral acceleration is required to be less then 0.1 m/s, therefore the weight on the acceleration was set to $W_{a_y} = 1/0.1$.

The maximal roll angle required is 45 deg. To normalize the roll commands so that $|\phi_{com}| \leq 1$ and to simulate the pilot's low frequency stick commands, the

roll command is prefiltered by

$$W_{pf} = \frac{45\pi}{180}\,\frac{s/100+1}{s/5+1}. \tag{24}$$

From the data presented at the beginning of this section, the payload mass changes in the range of ± 30 kg, with a nominal aircraft mass of 187 kg, i.e., the payload change constitutes $\pm 16\%$ of the nominal aircraft mass. The flight altitude changes between 0 and 10 Kft. In a standard atmosphere, the air density in this altitude range changes between 1.225 kg/m^3 and 0.879 kg/m^3. By designing the controller for a nominal altitude with an average air density, the relative change in air density is $\pm 17\%$. Normalizing the uncertainty of the mass and the air density such that $|\delta_\rho| \leq 1$ and $|\delta_m| \leq 1$, and since each of these uncertainties appears in a repeated scalar block of order three (Eq. 21), a weight on the uncertainty was set to

$$W_\Delta = \mathrm{diag}\,\{0.17I_3, 0.16I_3\} \tag{25}$$

The aircraft controls, the aileron and the rudder, have a maximal deflection angle of $\delta^{\max} = 20$ deg. The controls have a servo dynamics with a bandwidth of about 22 rad/sec, so high frequency control commands should be avoided. To reflect that, the weight on the controls was set to

$$W_\delta = \frac{1}{\delta^{\max}}\,\frac{s/20+1}{s/50+1}\begin{bmatrix} 1 & 0 \\ 0 & 1 \end{bmatrix} \tag{26}$$

The roll and yaw rate measurements contain an additive zero mean white noise with a standard deviation of $\sigma_n = 1$ deg/$\sqrt{\text{hour}}$, with no correlation between the roll rate noise and yaw rate noise. Thus the weight on the rates measurement noise was set to $W_n = \sigma_n I_2$. In a similar manner, the accelerometer measurement noise has a standard deviation of 0.01 m/$\sqrt{\text{sec}}$, and therefore $W_{n_{a_y}} = 0.01$.

The current μ design tools are not capable to perform μ controller synthesis for real uncertainties or repeated scalar blocks, though analysis of such blocks is possible. For this reason, the real repeated scalar blocks describing the mass and density uncertainties (Eq. 21) were replaced by six complex scalar blocks for synthesis purposes. This is essentially an over-bounding of the model uncertainty, forced by lack of numerical tools. However, after each stage of the design, a μ analysis with the exact uncertainty blocks was performed to check the quality of the synthesis. It was found that the difference between the all-complex μ and the mixed μ did not exceed 2% in the cases examined and where identical for the final results.

A robust μ controller was designed for the interconnection model of Fig. 2. The μ D-K iteration process[10] converged after 6 iterations to $\mu = 0.920$ with a 44^{th} order controller. The controller order was reduced using balanced truncation to order 29 with $\mu = 0.989$. The μ value less the unity means that all robust performance criteria were met for the specified uncertainties (variations) in the aircraft mass and the air density. Figure 3 demonstrates the closed loop response at several "edges" of the uncertainty space. It can be clearly seen that the closed loop response is hardly affected by the change in the aircraft mass and the air density, and the performance is within the required specifications. The design goals were achieved.

5 Autopilot Comparison

The controller in the previous section was based on the functional dependence model of the aircraft, as is reflected in Eq. (21), and will be referred to in the sequel as the μ_{FD} (Functional Dependence) controller. In order to evaluate this controller and demonstrate the importance and the advantages of including the functional dependence in the uncertainty model, a more common μ controller was designed. In the latter, the uncertainty model was constructed by bounding each parameter in the state space model separately.

The linear state space model of the aircraft was given in Eq. (10). This equation contains 17 parameters which are affected by the change in the payload mass and/or the air density. Each parameter was checked for its variations at the specified mass and air density range. Similar to the bounding rectangle in a two dimensional parameter space of the example in Fig. 1, here a bounding hyper-cube in a 17 dimensional parameter space is to be constructed. In Fig. 1, the rectangle bounded a curve created from a single unknown physical parameter. In the current example, the 17 dimensional hyper-cube bounds a surface created by the two unknown physical parameters.

A LFT containing 17 independent δ-s was constructed such that when the δ for a particular parameter is zero, the parameter receives its nominal value, and when $\delta = \pm 1$ the parameter receives its maximal or minimal value, respectively. As an example, suppose a is a parameter that changes between a_{min} and a_{max} with a nominal value of $\hat{a}$. The LFT for this parameter is

$$a = \mathcal{F}_l\left(\begin{bmatrix} \hat{a} & 2\,(a_{\max}-\hat{a})\,(a_{\min}-\hat{a}) \\ \dfrac{1}{a_{\max}-a_{\min}} & \dfrac{a_{\max}+a_{\min}-2\hat{a}}{a_{\max}-a_{\min}} \end{bmatrix}, \delta\right)$$

In a similar manner, a LFT was constructed for all parameters of Eq. (10) and the LFTs were then joined.

The interconnection model used for this controller is identical to that used in the μ_{FD} controller (Fig. 2.) The design specifications remained the same, except for the different 17^{th} order uncertainty model. This controller will be referred to as the μ_{PB} (Parameter Bounding) controller.

The design process converged after 5 D-K iterations to a value of $\mu_{\text{PB}} = 2.046$ with a 66^{th} order controller,

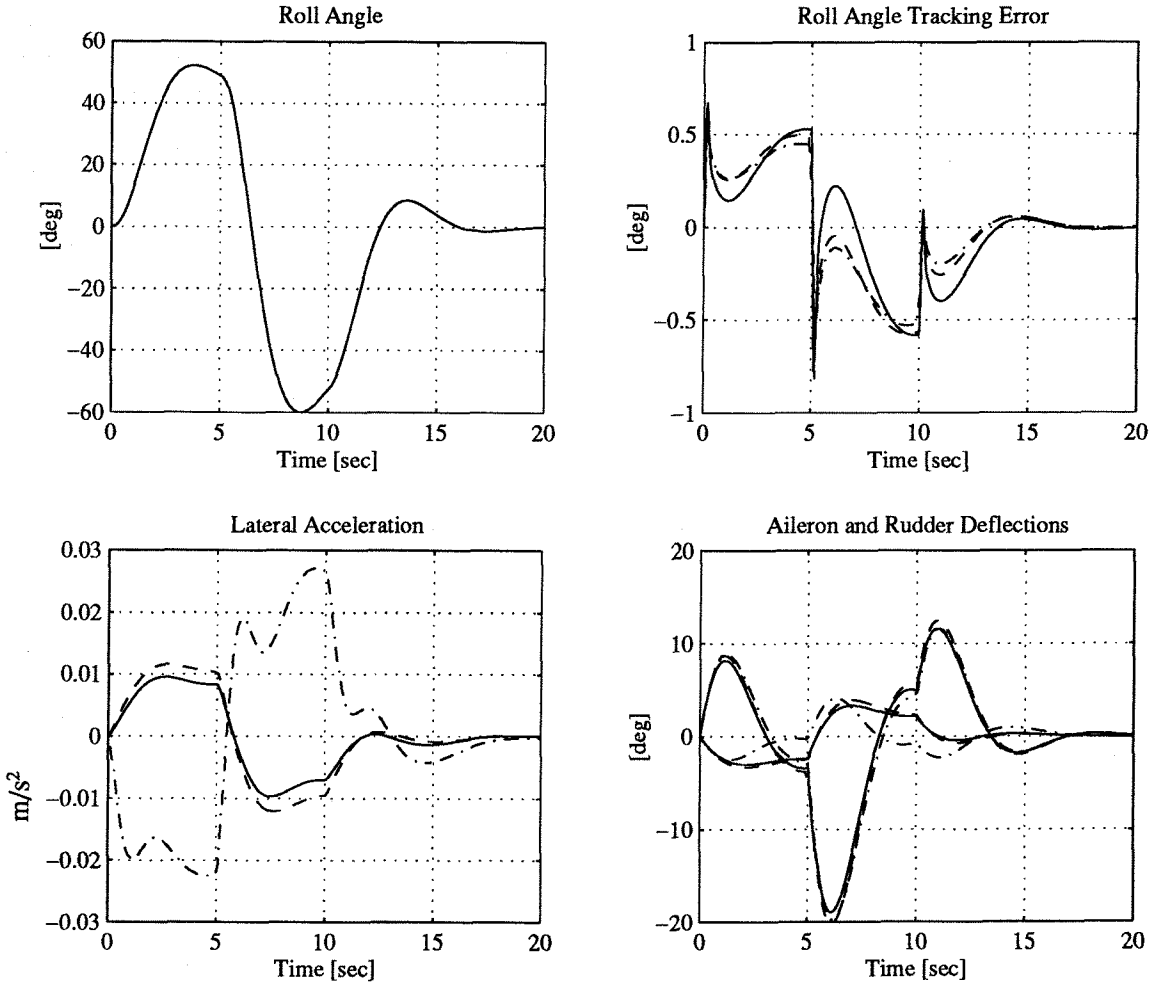

Figure 3: Lateral RPV Response with μ Controller. Solid line - ($\Delta m = 16\%, \Delta\rho = -17\%$); Dashed line - ($\Delta m = 16\%, \Delta\rho = 17\%$); Dash-Dot line - ($\Delta m = -16\%, \Delta\rho = 17\%$).

which was reduced to order 28 using optimal Hankel norm approximation[13] without affecting the μ value. The μ value in excess of unity indicates that the controller *does not* achieve the robust performance objectives considered by the PB model. However, since the PB model includes uncertainties which are not physical, it would be fair to compare the two controllers on the same uncertainty space - the physical uncertainty space. A μ analysis of the μ_{PB} controller using the FD model yielded $\mu_{\text{FD}} = 1.49$. Thus, the μ_{PB} controller *does not* provide robust performance even when considering only the physical uncertainties. Moreover, an analysis of the system within the μ_{PB} controller revealed that the controller does not even succeed in achieving stability for all the mass/density combinations in the uncertainty space.

A designer using only general parameter uncertainty bounds would conclude that a single controller cannot control the plant with the specified uncertainty range. As a resort, several controllers would have to be designed for a few subspaces of the complete uncertainty space, and a gain scheduling scheme would have to be set up. This is avoided by the functional dependence model.

The reason that the μ_{PB} controller doesn't provide the required performance and even has difficulties just stabilizing the system results from the fact that it is based on a *conservative* uncertainty model that contains non physical uncertainties. This controller has to cope with a larger uncertainty space, i.e., a larger possible plant group, and hence achieves a worse performance/robustness trade-off. This point is demonstrated in Fig. 4 which shows a two dimensional cross section of the parameter space. The parameters in the figure are normalized such that each parameter is nominally zero and has a maximal and minimal value of 1 and -1, respectively. The graph frame is essentially a projection of the 17 dimensional hyper-cube that bounds the uncertainty space for the PB model, since it bounds the parameters between their minimal and maximal values, independently. The gray area of the graph is the physical uncertainty space, i.e., for every value of

the parameters in the gray area there is a combination of mass and air density, within their uncertainty range, for which the parameters obtain the specified values. This area is actually a projection of the physical uncertainty surface onto the parameter space cross section. Using μ analysis it is possible to find the worst perturbation for the μ_{PB} controller, i.e., the perturbation of smallest size which caused the μ_{PB} controller to fail in meeting the performance requirements. This point is marked by a cross on the figure. As can be seen, this point occurs at a non physical combination of parameters. In other words, the μ_{PB} controller was given a larger plant group to control. Out of this group, the plant for which achieving the requirements was most difficult, is not a physical plant, i.e., it is not included in the group of plants which can occur by the actual physical uncertainties. Therefore, in order to design for the larger, more difficult, group of plants, the controller obtained a worse performance/robustness trade-off.

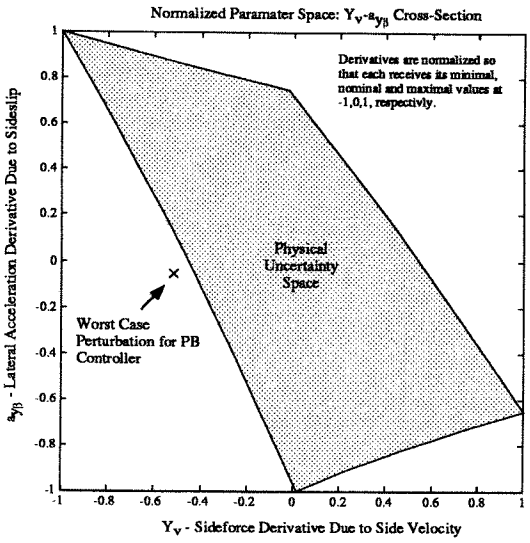

Figure 4: A Cross-Section in the Normalized Parameters Space

In summary, the μ_{PB} controller had to design against a larger plant group than is physical and hence against a much harder control situation than is necessary. This led to a bad performance/robustness tradeoff. In contrast, the μ_{FD}, which was designed while considering physical uncertainties only, was able to provide the required robust performance.

6 Summary and Conclusions

In this paper, an approach was presented to incorporate known functional dependencies of model parameters on uncertain physical quantities into the robust control design procedure. The approach is suitable in cases where the source of the plant uncertainty is mainly accountable by a few unknown physical parameters. Such is particularly the case in systems which are described by perturbation equations from distinct equilibrium states (trim conditions) like in aircraft flight dynamics equations.

The basis of the approach is to describe the uncertainties in the unknown physical values as Linear Fractional Transformations (LFTs). Then, using LFT algebra, a LFT is obtained, which describes the effect of the uncertain variables on the plant model by a single uncertainty block of a minimal dimension.

This procedure was demonstrated in a lateral autopilot design example. Here the controller was designed for a remotely piloted vehicle carrying payloads of unknown mass while flying at unknown altitude. Each of these uncertain variables changes the aircraft dynamic model parameters in a known fashion. The resulting model describes the plant uncertainty space without undesired over-bounding which would have occurred when treating the plant uncertainties without relating to their functional origins. A μ controller was designed using this model, which achieved robust performance in the specified uncertainty range.

For comparison, a μ controller was designed for the same performance specifications with an uncertainty model that did not use the functional dependence of the model parameters on the unknown physical variables. Instead, the model parameters were bound to reflect their uncertainties independently. The controller based on this model did not succeed to fulfill the required performance requirements and even failed to stabilize the system in the entire uncertainty range. An analysis showed that the most difficult case to control corresponded to a non physical combination of parameters. Had the functional dependence been incorporated to this model, the controller would not have had to cope against it. A designer using such a simple uncertainty description would have to reduce the performance requirements or to design several controllers for a few subspaces of the uncertainty space and establish a switching scheme between them. Often such "gain scheduling" can be avoided by using the functional dependence of the system parameters and thus considering physical uncertainties only.

The example clearly demonstrates the advantages of including the functional dependencies of the model parameters in the uncertainty model. The resulting model avoids uncertainty over-bounding and leads to a favorable controller design setup and superior robustness/performance trade-off.

Acknowledgement

The authors would like to acknowledge IAI for providing the RPV data used in this paper.

Appendix

The matrix M'_{lat} of Eq. (21) is partitioned as:

$$M'_{lat} = \left[\begin{array}{c|c} M'_{11} & M'_{12} \\ \hline M'_{21} & M'_{22} \end{array}\right]$$

and the submatrices are:

$$M'_{11} = \begin{bmatrix} -.1549 & 0 & -1 & .2453 & 0 & .0504 \\ -17.42 & -9.265 & 3.018 & 0 & 24.99 & 1.225 \\ 13.62 & .2529 & 1.074 & 0 & -1.847 & -8.707 \\ 0 & 1 & 0 & 0 & 0 & 0 \\ -.1549 & 0 & -1 & .2453 & 0 & .0504 \\ 0 & 1 & 0 & 0 & 0 & 0 \\ 0 & 0 & 1 & 0 & 0 & 0 \end{bmatrix}$$

$$M'_{12} = \begin{bmatrix} 1 & 0 & 0 & 1 & 0 & 0 \\ 0 & 1 & 0 & 0 & 1 & 0 \\ 0 & 0 & 1 & 0 & -7.108 & 0 \\ 0 & 0 & 0 & 0 & 0 & 0 \\ 1 & 0 & 0 & 0 & 0 & 1 \\ 0 & 0 & 0 & 0 & 0 & 0 \\ 0 & 0 & 0 & 0 & 0 & 0 \end{bmatrix}$$

$$M'_{21} = \begin{bmatrix} -.1151 & 0 & 0 & 0 & 0 & .0393 \\ -8.818 & -6.9161 & 3.068 & 0 & 14.07 & .6467 \\ 6.909 & -.0402 & -.8632 & 0 & -1.121 & -4.597 \\ .1151 & 0 & 0 & 0 & 0 & -.0393 \\ -.0416 & 0 & 0 & 0 & 0 & .0142 \\ -10.98 & .0645 & 1.386 & 0 & 1.800 & 7.343 \end{bmatrix}$$

$$M'_{11} = \begin{bmatrix} 0 & 0 & 0 & 0 & 0 & 0 \\ 0 & 0 & 0 & 0 & 0 & 0 \\ 0 & 0 & 0 & 0 & 0 & 0 \\ -1 & 0 & 0 & -1 & 0 & 0 \\ .3616 & 0 & 0 & 0 & -1 & 0 \\ -1 & 0 & -1.606 & 0 & 11.42 & -1 \end{bmatrix}$$

References

1. J. Ackermann. *Multi-Model Approaches to Robust Control System Design*, volume 70 of *Lecture Notes in Control and Information Sciences*. Springer-Verlag, May 1985.
2. P. Voulgaris and L. Valavani. High Performance Linear-Quadratic and H_∞ Designs for a Supermaneuverable Aircraft. *Journal of Guidance, Control, and Dynamics*, 14(1):157–165, Jan.–Feb. 1991.
3. W. Rogers and D. Collins. X-29 H_∞ Controller Synthesis. *Journal of Guidance, Control, and Dynamics*, 15(4):962–967, July–Aug. 1992.
4. J. Doyle, K. Lenz, and A. Packard. Design Examples Using μ Synthesis: Space Shuttle Lateral Axis FCS During Reentry. In *IEEE Conference of Decision and Control*, pages 2218–2223, Dec. 1986.
5. J. Reiner, G. Balas, and W. Garrard. Design of a Flight Control System for a Highly Maneuverable Aircraft Using Robust Dynamic Inversion. Journal of Guidance, Control, and Dynamics, Submitted April 1993.
6. A. Sparks and S. Banda. Application of Structued Singular Value Synthesis to a Fighter Aircraft. *Journal of Guidance, Control, and Dynamics*, 16(5):940–947, Sep.–Oct. 1993.
7. M. Idan and G. E. Shaviv. Robust Control Design Strategy with Parameter Dominated Uncertainty. In *AIAA Guidance, Navigation and Controll Conference*, pages 164–174, Baltimore, MD, Aug. 1995. To appear in *Journal of Guidance, Control, and Dynamics*, 19(3), May-June 1996.
8. J. C. Doyle, A. Packard, and K. Zhou. Review of LFTs, LMIs and μ. In *IEEE Conference of Decision and Control*, pages 1227–1232, Dec. 1991.
9. W. Wang, J. Doyle, C. Beck, and K. Glover. Model Reduction of LFT Systems. *IEEE Conference of Decision and Control*, pages 1233–1238, Dec. 1991.
10. A. Packard and J. Doyle. The Complex Stuctured Singular Value. *Automatica*, 29(1):71–109, Jan. 1993.
11. D. McRuer, I. Ashkenas, and D. Graham. *Aircraft Dynamics and Automatic Control*. Chapter 4, Princeton University Press, New Jersey, 1973.
12. D. McLean. *Automatic Flight Control Systems*. Chapters 2-4, Prentice Hall International (UK) Ltd, Cambridge, GB, 1990.
13. K. Glover. All Optimal Hankel Norm Approximations of Linear Multivariable Systems and their L^∞-Error Bounds. *International Journal of Control*, 39(6):1115–1193, Nov. 1984.